Available online at www.sciencedirect.com
ScienceDirect
Journal of Process Control 17 (2007) 253–260
JOURNAL OF PROCESS CONTROL
www.elsevier.com/locate/jprocont

Modelling of HIV infection: Vaccine readiness, drug effectiveness and therapeutical failures

Xiaohua Xia *

Department of Electrical, Electronic and Computer Engineering, University of Pretoria, South Africa

Received 10 July 2006; received in revised form 6 October 2006; accepted 23 October 2006

Abstract

A review of mathematical models for the pathogenesis of HIV is presented. Model identifiability and identification techniques are applied using the biomedical model and clinical data. Identifiability analysis aids in the determination of measured values and measurement frequency. Parameter identification methods are chosen and developed for sparse and rough samples. Results are reported on two case studies: vaccine readiness in Southern Africa, drug effectiveness and therapy failures on existing patients in France. Ongoing research programmes and future opportunities are considered.

Keywords: Biomedical; HIV/AIDS; Identifiability; Identification; Nonlinear systems

1. Introduction and a review of HIV models

The key markers of the disease progression due to the human immunodeficiency virus (HIV) and the acquired immunodeficiency syndrome (AIDS) are the CD4+ T-cell and viral levels in the plasma. A typical dynamics of the disease progression in an untreated individual is shown in Fig. 1 [8]. Highly active antiretroviral therapy (HAART), therapeutic regimens employing drug combinations has shown its ability to cause dramatic and sustained suppression of viral replication and immune system recovery. A typical patient's response is shown in Fig. 2 [14].

A basic 3D model [24] has been developed to reveal the dynamics in these figures:

$$\begin{cases} \dot{T} = s + rp(T,v) - dT - \beta Tv, \\ \dot{T}^* = \beta Tv - \mu T^*, \\ \dot{v} = kT^* - cv, \end{cases} \tag{1}$$

where T denotes the healthy CD4 cells, T^* denotes the infected CD4 cells, v denotes the free virus particles. Free virus particles infect uninfected cells at a rate proportional to the product of their abundances, βvT. Infected cells produce free virus at a rate proportional to their abundance, kT^*. Infected cells die at a rate μT^*, and free virus particles are removed from the system at rate cv. The total amount of virus particles produced from one infected cell, the "burst size", is k/μ. The simplest assumption is that uninfected cells are produced at a constant rate, s, and die at a rate, dT, and $p(T,v)$ denotes the proliferation of the CD4 cells.

It is estimated that as many as 10^{10} virions are produced and destroyed in an infected individual each day [31]. These findings are consistent with a simple steady-state analysis of the model (1) (see Ref. [30]). The equilibrium of virus depicted by the model (1) is

$$v^* = \frac{ks}{\mu c} - \frac{d}{\beta}. \tag{2}$$

Medical doctors use a term of "set-point" to represent the relative steady viral level during the asymptomatic stage of an HIV infection. This corresponds to the equilibrium (2). Throughout this paper, we will use the term "set-point" in this sense.

* Tel.: +27 12 420 2165; fax: +27 12 362 5000.
E-mail address: xxia@postino.up.ac.za

0959-1524/$ - see front matter © 2006 Elsevier Ltd. All rights reserved.
doi:10.1016/j.jprocont.2006.10.007

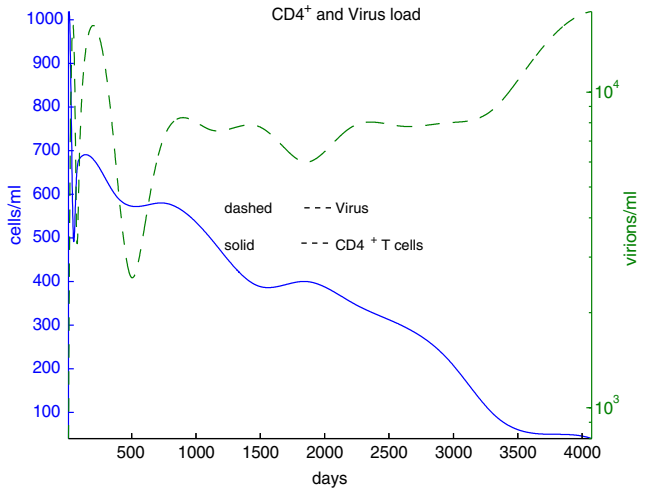

Fig. 1. Typical HIV/AIDS course [8].

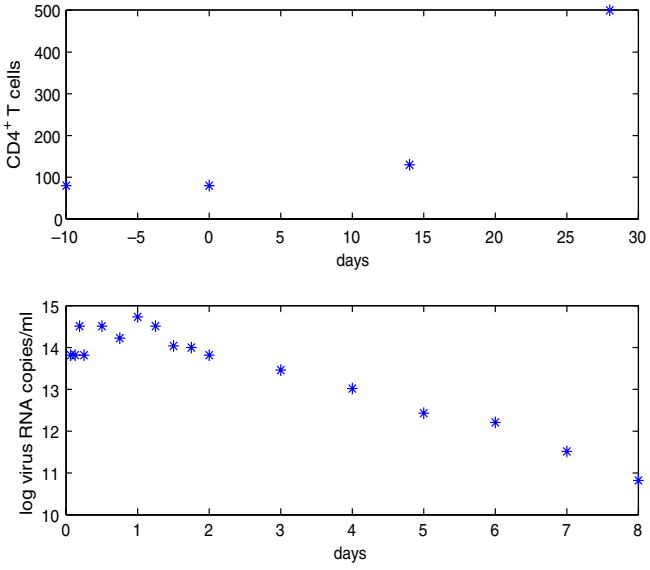

Fig. 2. Typical post-treatment dynamics [14].

It can be seen that a model of such a simple nature is able to adequately reflect the disease progression from the initial infection to an asymptomatic stage where the set-point is reached. This is one of the reasons why this model was used in the estimation of set-points in the vaccine programme [11,10] (see also Section 3.1).

One of the interpretations of antiviral drugs, reverse transcriptase inhibitors (RTI) and protease inhibitors (PI) in particular, is that they reduce infection of healthy cells [23]. Under an ideal situation, a 100% effective inhibitor corresponds in the model to setting $\beta = 0$. This understanding has yielded estimates for μ and c in Ref. [31] at roughly 0.45/day and 3/day, respectively.

The pool of virus producing cells has been estimated to be very small (3×10^7 [2]). If there are no other sources of hidden virus, the eradication of all the virus would take only about 25 days ($3 \times 10^7 \exp(-0.45 \times 25) < 1$).

Even though the basic model is only valid for a short period of the disease progression, researchers still use it to explain the hallmark long term depletion of CD4+ T-cells [1]. The prolonged, high level output of HIV *in vivo* reflects an active, ongoing, process in which CD4 lymphocytes are being infected and killed in large numbers.

Perelson et al. observed that, after the rapid first phase of decay during the initial 1–2 weeks of antiretroviral treatment, plasma virus levels declined at a considerably slower rate. This second-phase of viral decay was attributed to the turnover of a longer-lived virus reservoir of infected cell population, which can be adequately described by a long-lived cell model.

A latently infected cell model was also proposed, because additional cellular reservoirs of virus were found in lymphoid tissues [13], particularly on the surface of follicular dendritic cells (FDC). The source underlying the second-phase kinetics might be the release of virions trapped in the lymphoid tissues. It could be linked to infected macrophage, and/or due to the activation of latently infected cells.

The long-lived cells were determined to have a half-life of 1–4 weeks. This means that on average it would take between two and a half to 3 years of perfectly effective treatment to eradicate the virus. This estimate generated significant enthusiasm and optimism in 1996 [28]. As it turned out that a third-phase of HIV decay was observed from continued study of persons who had remained on HAART for extended periods of time. This study suggested that there possibly exists a reservoir of long-lived CD4+ memory T-lymphocytes [30]. The kinetics of decay are extremely slow, and the half-life of the memory cell reservoir has been estimated at between 6 and 44 months. As a consequence, the predicted time required for effective antiretroviral therapy to fully eradicate HIV from the body ranges from 9 to 72 years. It implies that conventional antiretroviral regimens are not a true virologic cure. Table 1 is a summary of these important findings. Most of information can be found or deduced from Ref. [7].

The above theories and models are the results in only one direction of the research devoted to addressing some deficiencies of the basic model (1). The above description does not cover all the known model deficiencies, nor does it exhaustively list all models developed to address the drawbacks. For example, a totally different theory proposed by Grossman and colleagues says that the very slow rates of viral decline which occur following initiation of HAART can be best explained if most of the virus is produced by cells infected *after* the commencement of treat-

Table 1
Virus reservoir and life span

Infected cell	Size	Half-life	Eradication
Active CD4	3×10^7	1 day	25 days
FDC	3×10^8–10^{11}	1–4 weeks	0.5–2.8 yr
Macrophage	n.a.	1–4 weeks	n.a.
Memory CD4	10^5–10^6	6–44 months	9–72 yr

ment. [12]. A few multi-compartment models [3,29] were proposed to reveal virus trafficking between different compartments. Another model by Ref. [18] was to capture the altered lymphocyte circulation patterns between the lymph system and blood due to HIV-induced enhanced lymph-node homing and subsequent apoptosis of resting CD4+ T-cells. The cytotoxic T-lymphocytes (CTL) models [19,22] deal with the interactions between viruses and immune response. The quasi species models of viral dynamics explore the effect of mutation of virus replication and the emergence of drug resistance. There are also models about antigenic variations in single and multiple epitopes [25]. Stochastic models [34] offer alternatives to look at the infection and progression of the disease. Refer to [4] for some of the early models, and [30,24,1] for other important models. Refer to Ref. [37] for some of the newest models.

These developments have brought researchers to face a number of challenges. It is clear that the modelling approach has paved the way for theoretical research and has changed the perception of people about the disease. This is achieved by extracting key features from the model parameters. Researchers using mathematical models often assume the process act deterministically, such that accurate models will precisely describe the evolution of the infection and disease. This approach, fundamentally different from the "orthodoxical" medical approach based on statistics over large population, relies on a rapid collection of individual patient's data over a short period of time. Even though there are general observations that can be made from the model and its structure, it is only when the model is tailored to each patient's individual parameters that clear benefits in the treatment strategy arise. More complex models involve more variables, and thus need more data. The records of patients in current clinical practise are typically sparse and rough. There is a need to strike a balance in model complexity and usability in order to use the HIV/AIDS models as a tool for treatment decisions. The purpose of this article is to put together some of the work on the HIV model building by taking into consideration of limited and poor data available in current clinical practise. The following sections show applications of some simple models. Control engineering techniques are used for model development.

2. HIV/AIDS parameters

In this Section 2, it will first be shown how an identifiability study of some simple HIV/AIDS models helps in formulating guidelines for clinical testing and measurement. Some parameter estimation methods will be described.

2.1. Identifiability

For identification of HIV/AIDS model parameters, the measured variables must first be determined. Clinically, many variables can be measured, though some of them with limited accuracy and high cost. The clinical practise recommended by some medical guidelines [35] is to measure the viral load and the CD4+ T-cell counts in plasma. Since CD4+ T-cells are predominantly healthy cells [15], also for technical reasons (see [38]), it is assumed that viral load and healthy CD4+ T-cells are measured outputs.

The following questions then arise: What is the minimal number of measurement samples for the CD4+ T-cell and the viral counts? When should these measurements be taken? Can one determine accurate estimates of model parameters from these measurements?

Identifiability is a basic system property to address these questions. To illustrate this, and for simplicity consider (1) with the proliferation term, and take the outputs as

$$\begin{aligned} y_1 &= T, \\ y_2 &= v, \end{aligned} \tag{3}$$

the system (1) is identifiable, as was shown in [39]. The system (1) has six parameters, denoted by

$$\chi = (s, d, \beta, c, \mu, k)^T.$$

Identifiability or precisely, algebraic identifiability [39], means that all parameters χ can be determined from the measured output. To actually find the parameters, higher order differential equations of the output can be calculated:

$$\dot{y}_1 = \theta_1 + \theta_2 y_1 + \theta_3 y_1 y_2, \tag{4}$$

$$\ddot{y}_2 = \theta_4 \dot{y}_2 + \theta_5 y_2 + \theta_6 y_1 y_2, \tag{5}$$

where $\Theta = (\theta_1, \theta_2, \theta_3, \theta_4, \theta_5, \theta_6)^{\mathrm{T}} = (s, -d, -\beta, -\mu - c, -\mu c, k\beta)^{\mathrm{T}}$. Θ defines a one-to-one map for $\beta \neq 0$ and $c > \mu$ [24]. Therefore, the identification of the original parameters of Eq. (1) is equivalent to that of Θ. Thus, all the original parameters are identifiable from the measurement of the viral load and the CD4+ T-cell counts in the blood of an HIV patient.

It is necessary to generate a minimum of six equations based on (4) and (5), three from each equation. This can be achieved by differentiating Eqs. (4) and (5) two more times, resulting in derivatives of y_1 and y_2 up to the order of 3 and 4, respectively. To cope with these order of derivatives, one concludes that at least four measurements of the CD4+ T-cell count y_1 and five measurements of the viral load are needed for a complete determination of all the HIV/AIDS parameters in the three-dimensional model (1). Identifiability of other models, and with different measured outputs, is studied in [39,17,16].

2.2. Parameter estimation

2.2.1. Least square estimates

For simplicity, assume that measurements y_1^0, y_1^1, y_1^2, y_1^3, y_2^0, y_2^1, y_2^2, y_2^3, and y_2^4 are available (the superscripts denote sample numbers), the following three equations can be generated based on Eq. (4), in which the derivative of y_1 is approximated by $\Delta y_1/\Delta t$:

$$A\begin{bmatrix}\theta_1\\ \theta_2\\ \theta_3\end{bmatrix}=\begin{bmatrix}1 & y_1^0 & y_1^0y_2^0\\ 1 & y_1^1 & y_1^1y_2^1\\ 1 & y_1^2 & y_1^2y_2^2\end{bmatrix}\begin{bmatrix}\theta_1\\ \theta_2\\ \theta_3\end{bmatrix}=\begin{bmatrix}\frac{y_1^1-y_1^0}{d_1}\\ \frac{y_1^2-y_1^1}{d_2}\\ \frac{y_1^3-y_1^2}{d_3}\end{bmatrix}.$$

If the matrix A is nonsingular, then there is a unique solution for θ_1, θ_2 and θ_3, and hence estimates for s, d and β. These are essentially least square (LSQ) estimates.

On the other hand, when either y_1 or y_2 is constant, A can never be nonsingular for any choice of measurement interval. In the long asymptomatic stage, the viral load y_2 remains constant, and in the short period after chemotherapy treatment, the CD4+ T-cell count does not change significantly (see the assumptions made in [14,36]). Therefore during these two time periods, a complete determination of s,d and β is impossible. Similar conclusions can be drawn from working with Eq. (5) for the estimates of μ, c and k.

This analysis also helps to indicate the most likely period for a complete estimation of parameters. An intuitive interpretation of the above analysis is that when the rate of change of y_1 and y_2 are sufficiently rapid and the cumulative strength of the virus (y_2) is bounded, all six parameters can be estimated with confidence. Two typical such phases in HIV/AIDS progression are the primary infection stage and the period after chemotherapy treatment when both the viral load and CD4+ T-cell counts are changing.

Coincidentally, one notices that all previous estimations of the virus clearance rate (c) and the death rate of infected cell (μ) were made for a post-treatment period of very strong chemotherapy with reverse transcriptor inhibitors and protease inhibitors in Refs. [14,36,31]. This choice becomes obvious from the above analysis of parameter convergence.

Of course, this pure LSQ would fail with noisy measurements. The measurement error of the Roche Amplicor assay method could be 0.18 log10 copies/ml [33]. Another problem with the pure LSQ is that the measurements of viral load and CD4 cells have to coincide in time. Ways to overcome these include adaptive algorithms [38] and improved versions of the LSQ method.

2.2.2. A penalty function approach

The penalty function method is in essence LSQ based, but with two important differences: firstly, derivative estimation is only present when a nominal curve is generated by a numerical ordinary differential equation solver and, thus, this estimation is not influenced by measurement noise. Secondly, the cost function is not limited to the LSQ distance, thus, it can be expanded to accommodate a diverse base of knowledge in order to increase the accuracy of parameter estimation.

In addition, since the penalty function method does not require any product terms, there is no constraint on the length of CD4+ T-cell and virus data vectors. Together with N measurements of T and K measurements of v, at time $t_1,\ldots,t_N$, and $\tau_1,\ldots,\tau_K$, respectively, the basic cost function is defined as

$$J_w=\sum_{n=1}^{N}\frac{(\widehat{T}(t_n)-T_n)^2}{N\ \mathrm{mean}(T_n)}+\sum_{k=1}^{K}\frac{(\hat{v}(\tau_k)-v_k)^2}{K\ \mathrm{mean}(v_k)}.$$

It can been seen that the points of the two data vectors need not coincide in time.

Additional refinements of the cost function can be made incorporating outside knowledge of the data set and the parameters. For example,

$$J_r=J_w+\kappa_1\ \max\left(\frac{\mathrm{d}\hat{v}_s}{\mathrm{d}t},0\right)+\kappa_2\ \max(\hat{\mu}-\hat{c},0),$$

where $\hat{v}_s$ is the vector of computed viral load, truncated after a few days. κ_1 and κ_2 are two scaling constants. The first refinement term corresponds to the knowledge that the patient is in steady-state before initiation of therapy. The second refinement term corresponds to the statement that the average infected CD4+ T-cell lives longer than free virions.

To validate the method, the parameter estimation for the three patients in Ref. [30] was repeated in ref. [9]. It was used to extract the same two parameters as in the experiment. Note that all the assumptions described in the experiment were included in the estimate by customizing the penalty function as described above. The results are listed in Table 2 for patient number 107 whose data was plotted in Fig. 2.

There is a distinct, and consistent difference in $\hat{c}$ between the published results and the estimation by custom penalty function. Since the estimation of c is dependent on the shoulder region of the virus count [24], a dependence on x_0 is to be expected. For an optimal adjusted x_0, one can estimate the parameters again with the same cost function. The small data window for this experiment does not allow clear information to be found about the initial conditions. It is clear from the results that the estimation of c, and to a lesser extent, of μ, is dependent on outside information about x_0.

2.2.3. A deterministic optimization method

To speed up the calculation, [27,26] employed an estimation procedure applied to the discrete-time model of the system (1). The principle of the estimation procedure is explained as the following. Suppose an optimization algorithm (e.g., steepest descent, simplex) is chosen. Running this algorithm to minimize an objective function on large number of initial conditions, one can see that the solutions are distributed in the neighborhood of the real optimum. A

Table 2
Comparisons of estimates

Patient no.	Method	$\hat{c}$ (day^{-1})	$t_{c\frac{1}{2}}$ (days)	$\hat{\mu}$ (day^{-1})	$t_{\mu\frac{1}{2}}$ (days)
10^7	published	3.1	0.2	0.5	1.4
penalty	function	2.07	0.33	0.50	1.39
x_0	*modified*	*3.07*	*0.23*	*0.49*	*1.41*

median and an interquartile range (IQR) of the calculated solutions offer a desired estimate and the confidence interval of the estimate. Since a deterministic approach is taken, the procedure is called a deterministic optimization method.

The IQR measures the dispersion of the results. It depends on the used tolerance and the convexity of the objective function. The IQR gives an important information on the confidence on the results. This method is extremely useful with sparse data samples. In the HIV/AIDS case, for ethical and financial reasons, it is impossible to collect large amount of data. With the deterministic optimization method, [27,26] were able to compute estimates of all the parameters of the model (1) with minimum number of samples.

3. Case studies

3.1. HIV vaccine readiness

An interesting application of the estimation procedures, described in Section 2.2.2, is the extraction of parameters for patients who took part in an HIV/AIDS vaccine readiness study [11]. In this study, HIV viral load may be a critical endpoint in vaccine trails by which to judge efficacy. It is important to define viral dynamics in unvaccinated infected individuals, especially in non-B subtype infections where little information is available. HIV-B subtype viruses are prevalent in North America, Europe and Australia. HIV-non-B subtypes prevalent elsewhere in the world differ from subtype B in the envelope gene by as much as 30%. The main aim was to determine the set-point for these patients,and find the time from seroconversion (detectable HIV antibodies) for this set-point to be reached.

Fifty-one individuals with recent HIV infection were recruited within 18 months of acquiring HIV infection from fourP countries in southern Africa (10 from Zimbabwe, 6 from Malawi, 16 from Zambia and 19 from South Africa). Participants were followed at 2, 4, 7 and 9 months after enrolment. At each visit, blood samples were obtained for plasma RNA levels, lymphocyte subset analysis and DNA isolation. Participants were not on antiretroviral treatment.

The majority (42/51) were female. The median age was 28 and the median interval from seroconversion to first viral load measurement was 8.9 months (interquartile range of 5.5–14.1). Comparison of $\log_{10}$RNA copies/ml in participants at enrolment between countries showed no significant difference and, based on this, were grouped as one cohort.

Quite coincidentally, 34 of the 51 participants had 4 CD4+ T-cell and 5 viral load counts, thus satisfying the minimum requirement of algebraic identifiability of the basic model. Ten additional patients from the cohort had insufficient data points for a complete evaluation of parameters on their own. For these patients, the assumption was made that their parameter value for c, the death rate constant for virus, did not differ significantly from other patients in the cohort. The rest of the data (of seven patients) have too few samples to be useful. Thus, in total, parameters were estimated for 44 of the 51 participants. Typical data sets are displayed in Table 3 for two patients P15 and P42.

Table 3
Data points for two sample patients

Days P 15	Viral load (5 + 4)	CD4+ P 42	Days	Viral load (4 + 3)	CD4+
391	46699		411	67813	
426	24463	187	474	11569	
503	62364	136	586	39887	186
573	25079	193	685		178
636	29821	143	775	19359	272

Even though the minimum requirements for parameter estimation were met by most of the patients in this study, the time difference between points, lack of initial CD4+ T-cell data and imprecise measurements, required a set of assumptions to be made before the model parameters were estimated: (i) patients were in the early stages of infection; (ii) the midpoint between the last negative and first positive sample was taken as an estimate for the time of seroconversion; (iii) patients did reach a steady-state in viral load; (iv) initial values for the viral load coincided with the first viral load measurement; (v) the order of c and μ was not dictated in this instance of the cost function; (vi) others (for details and a discussion of these assumptions, see [9,10]).

After the parameters for each patient had been estimated, the set-point was calculated according to (2). In order to find the time to reach the set-point, the fluctuations in viral load were considered. The time from seroconversion to the point where the fluctuations fell within $\log 0.5$ of the set-point was taken as an estimate for the time to reach set-point.

In Fig. 3 a detailed view is given for P42 with four data points in the viral load. The markers indicate data points and the corresponding model prediction (solid line), derived from parameter estimates. The estimation of the set-point is indicated by a dashed line, and the time to set-point is taken at the point where the modelled viral load falls between the dotted lines.

The sparsity of the data set did not allow a conclusion about an individual patient, but the results of 44 patients can provide some statistical information about subtype C (predominantly in Southern Africa and India) viral dynamics. The following median estimates of parameters were found

$$\hat{\chi} = (7.48, 0.00085, 1.4 \times 10^{-6}, 1.56, 0.80, 2834)^T.$$

Fig. 4 shows the normal probability plot of $\log_{10}$ set-point estimations for all patients. It is clear that the estimates follow a log–normal distribution. The Bera–Jarque parametric hypothesis test of composite normality confirms this, with a significance level of 0.298. The calculated median

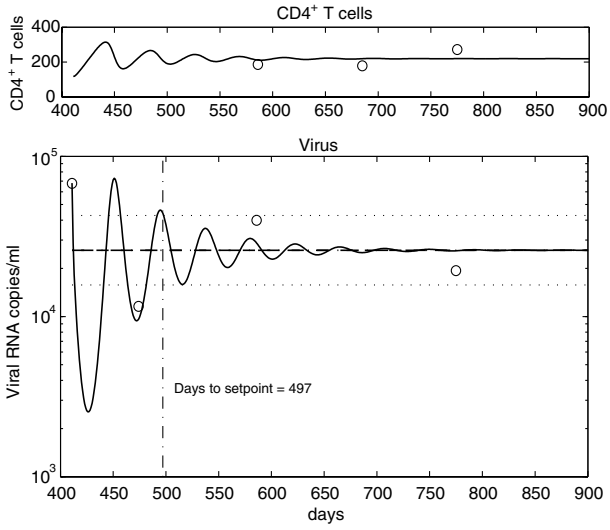

Fig. 3. Model and data example [10].

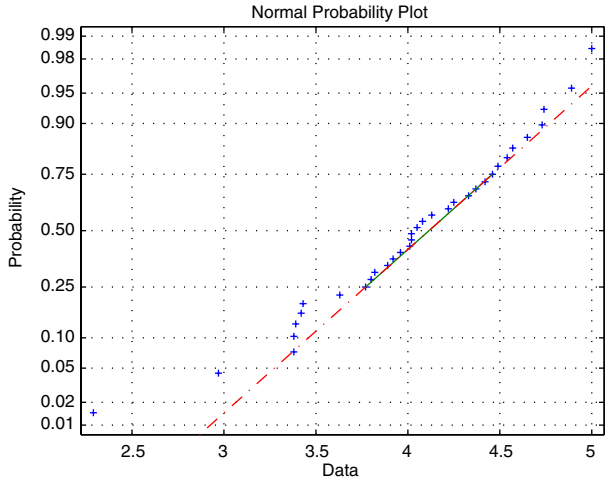

Fig. 4. Normal probability plot of set-point estimations [10].

time to set-point was 16.57 months and the median of the calculated set-point distribution was $4.08\log_{10}$ (12143 RNA copies/ml). Interestingly, these estimates appear to be no different from reported studies of subtype B HIV infected male cohorts [20,21,32].

3.2. Therapy effectiveness and therapeutical failures

In another case study, parameter estimates were obtained using the deterministic optimization method for two representative patients from the CHU of Nantes, France (Nantes University Hospital).

The first patient was 43 years of age. He was treated in two consecutive periods. In the first period from day 0 to day 272, the patient was treated with two RTIs: zidovudine (AZT) and lamivudine (3TC) and one PI: saquinavir soft gel (SQV). During this period, the viral load drops from 65 000 copies/ml to 5000 copies/ml in 113 days, and then increases to 21 000 copies/ml. In the second period from day 273 to day 2379, the patient's therapy consists of two RTIs: 3TC and stavudine (d4T) and one PI ritonavir (ABT-538). The viral load drops under the threshold of 50 copies/ml.

The second patient was 42 years old. The first line of antiretroviral therapy is a bi-associated combination of RTI (AZT+3TC): from day 0 to day 124, then a tritherapy, AZT +3TC+IDV (indinavir), for the next 769 days. During the second period, the patient received several associations: AZT+3TC+ABT-538+IDV (treatment stopped by the patient's decision); AZT+3TC+NFV (nelfinavir) (treatment stopped due to a virological failure); AZT+3TC+IDV (treatment stopped for toxicity). All these therapies have not been shown to be efficient. In the last period, the patient is treated with AZT +3TC +EFV (efavirenz). No PI was involved.

In the parameter estimation, it was assumed that the proliferation term in (1) takes the following form $p = rTv/(K+v)$.

Two thousand initial conditions were used, and they were assumed to be uniformly distributed on an admissible interval of the underlining parameter. For example, the admissible interval was chosen to be $[10^{-20}, 20]$ assuming that the production of CD4 cells is always positive and smaller than 20 CD4/mm^3.

One should note that parameters are patient dependent. The estimates for patient 2 are tabulated in Table 4, in which estimates outside of brackets are for the first period, and estimates in brackets (...) are for the period from day 1280 to day 2388.

From these results, it can be observed that for patient 2 and in the second period of treatment, the parameter β increases (1450 times higher), and k decreases by 9 times lower than that in the first period. This implies that the AZT+3TC+EFV combination is more efficient than the

Table 4
Estimates of patient 2

	Estimates	IQR	$CI_{50\%}$
s	0.46 (0.13)	0.57 (0.24)	[0.13,0.17] ([5.55×10^{-4}, 0.24])
d	2.09×10^{-3} (2.79×10^{-3})	3.68×10^{-3} (6.78×10^{-3})	[8.44×10^{-5}, 3.77×10^{-3}] ([4.30×10^{-4}, 7.20×10^{-3}])
μ	0.06 (0.12)	0.037 (0.1)	[0.044, 0.074] ([0.079, 0.18])
c	0.092 (0.64)	0.068 (0.97)	[0.061, 0.13] ([0.3, 1.26])
β	1.02×10^{-9} (1.50×10^{-6})	1.79×10^{-8} (2.13×10^{-6})	[5.42×10^{-14}, 1.79×10^{-8}] ([6.19×10^{-7}, 2.75×10^{-6}])
k	2604 (296.24)	5186.5 (604.73)	[152.04, 5338.5] ([102.21, 706.94])
r	1.08×10^{-4} (3.23×10^{-3})	8.04×10^{-3} (7.75×10^{-3})	[2.79×10^{-9}, 0.008] ([1.04×10^{-5}, 7.76×10^{-3}])
K	9.53 (17.36)	1009 (146.5)	[3.59×10^{-5}, 1009] ([0.087, 146.59])

AZT+3TC combination in the first period. The lack of PI results in higher value of the parameter β. The higher value of r suggests a more active proliferation in the second period. It could also be recommended that the RTIs of the second period (AZT+3TC+EFV) combined with the PI of the first period (IDV) could further lower both parameters β and k.

Virological failure is due to persistent replication of the viral load under treatment. Thus virological failure could be interpreted as extreme values of the parameters k and β. Immunological failure is defined when the amount of CD4 cells remains below the level of 200/mm^3 after 6 months of treatment. Immunological failure could be detected by the indicator:

$$t_{200} = \frac{1}{\tilde{d}}\left[-\log_e\left(1 - 200\frac{\tilde{d}}{s}\right) + \log_e\left(1 - \frac{\tilde{d}}{s}T_0\right)\right],$$

where $\tilde{d} = d - \frac{r\bar{v}}{K+\bar{v}}$, $\bar{v}$ is the mean of the viral load, and T_0 is the initial CD4 cell level. If $t_{200} > 6$ months, then there is immunological failure.

It could be verified that $t_{200} = 33$ months, indicating an immunological failure of the first period of treatment on patient 2. Clinical data shows that approximately 25 months were necessary for him to reach the 200 CD4/mm^3 level.

A superposition of both virological and immunological failure is referred to as biological failure, and clinical failure is characterized by the clinical manifestation of opportunistic diseases.

4. Concluding remarks

The research of the pathogenesis of HIV has reached a point where control system engineering can play a constructive role. The parameter estimation schemes are also useful for immune prognosis. Anti-retroviral therapies are usually effective in suppressing the viral load in a short period of time. The response of immune systems takes a longer time (usually more than a month) to manifest. In current clinical practice, immune responses are usually monitored after 6 months after treatment. It is desirable to predict the immune system response with less than a month's samples. Preliminary results in this regard have been done for six naive patients at CHU of Nantes, France, and further experiments are currently done for more difficult patients.

A large amount of raw data have been accumulated around the world of HIV patients under HAART. The drug effectiveness and therapeutical failure models have to be populated with different HIV subtypes and with different geographic data. For this purpose, an automated computer routine has the advantage, and is also under current investigation. The system modelling ideas can certainly be borrowed to HIV and TB co-infections and other infectious disease.

As can be seen from the case studies, one of the challenges from a parameter estimation's viewpoint is limited and poor data. Perhaps the biggest scientific open problem is whether a true cure for HIV/AIDS can eventually be found. If there is a cure, then one thing is certain that it comes as a treatment strategy which includes not only combination of drugs but also the manner in which these drugs are administered. From a practical point of view, affordable and effective means to prevent and stop infection and progression is the key to the success of the fight against AIDS. Applying these ideas to create suitable educational platforms for the high-risk groups of people is also deemed necessary [6,5].

Acknowledgement

I express my gratitude to all my collaborators on the research of HIV/AIDS for allowing me to use some materials from our joint publications and research.

References

[1] D.S. Callaway, A.S. Perelson, HIV-1 infection and low steady-state viral loads, Bulletin of Mathematical Biology 64 (2002) 29–64.
[2] T.W. Chun, L. Carruth, et al., Quantification of latent tissue reservoirs and total body viral load in HIV-1 infection, Nature 387 (1997) 183–188.
[3] G. Cocho, L. Huerta, et al., A multiple compartment model for the evolution of HIV-1 after highly active antiretroviral therapy, Mathematical Approaches for Emerging and Reemerging Infectious Diseases: an Introduction (Minneapolis, MN, 1999)IMA Journal of Mathematics Applied in Medicine and Biology, Vol.125, Springer, New York, 2002, 309–323.
[4] D. Covert, D. Kirschner, Revisiting early models of the host-pathogen interactions in HIV infection, Comments Theoretical Biology 5 (2000) 383–411.
[5] I. Craig, X. Xia, Can HIV/AIDS be controlled? IEEE Control Systems Magazine 25 (2005) 80–83.
[6] I. Craig, X. Xia, J.W. Venter, Introducing HIV/AIDS education into the electrical engineering curriculum at the University of Pretoria, IEEE Transactions on Education 47 (2004) 65–73.
[7] S. Dewhurst, R.L.W. da Cruz, L. Whetter, Pathogenesis and treatment of HIV-1 infection: recent developments (Y2K update), Frontiers in Bioscience 5 (2000) 30–49.
[8] A.S. Fauci, G. Pantaleo, S. Stanley, D. Weissman, Immunopathogenic mechanisms of HIV infection, Annals of Internal Medicine 124 (1996) 654–663.
[9] R. Filter, X. Xia, A penalty function approach to HIV/AIDS model parameter estimation, in: Proceedings of the 13th IFAC Symposium on System Identification, Rotterdam, The Netherlands, 2003. August 27–29.
[10] R. Filter, X. Xia, C. Gray, Dynamic HIV/AIDS parameter estimation with application to a vaccine readiness study in Southern Africa, IEEE Transactions on Biomedical Engineering 52 (2003) 284–291.
[11] C. Gray, C. Williamson, H. Bredell, A. Puren, X. Xia, et al., Viral dynamics and CD4+ T-cell counts in subtype C human immunodeficiency virus type-1 -infected individuals from southern Africa, Aids Research and Human Retroviruses 21 (2005) 285–291.
[12] Z. Grossman, M. Polis, et al., Ongoing dissemination during HAART, Nature Medicine 5 (1999) 1099–1104.
[13] A.T. Haase, K. Henry, et al., Quantitative image analysis of HIV-1 infection in lymphoid tissue, Science 274 (1996) 985–989.
[14] D.D. Ho, A.U. Neumann, et al., Rapid turnover of plasma virions and CD4 lymphocytes in HIV-1 infection, Nature 273 (1995) 123–126.

[15] C.A. Janeway, P. Travers, Immunobiology: The Immune System in Health and Disease, Garland, New York, 1997.
[16] M. Jeffrey, X. Xia, Identifiability of HIV/AIDS models, in: H. Wu and W.Y. Tan (Eds.), Deterministic and Stochastic Models of AIDS and HIV with Intervention, World Scientific Publications, Singapore (Chapter 11).
[17] M. Jeffrey, X. Xia, I. Craig, Identifiability of an extended HIV model, in: Proceedings of the 5th IFAC Symposium on Modelling and Control in Biomedical System, Melbourne, Australia, August 21–23, 2003.
[18] D. Kirschner, G.F. Webb, M. Cloyd, Model of HIV-1 disease progression based on virus-induced lymph node homing and homing-induced apoptosis of CD4+ lyphocytes, JAIDS 24 (2000) 352–362.
[19] P. Klenerman, R.E. Phillips, et al., Cytotoxic T-lymphocytes and viral turnover in HIV type-1 infection, Proceedings of the National Academic Science USA 93 (1996) 15323–15328.
[20] J.W. Mellors, C.R. Rinaldo, et al., Prognosis in HIV-1 infection predicted by the quantity of virus in plasma, Science 272 (1996) 1167–1170.
[21] J.W. Mellors, A. Munoz, et al., Plasma viral load and CD4+ lymphocytes as prognostic markers of HIV-1 infection, Annals of Internal Medicine 126 (1997) 946–954.
[22] M.A. Nowak, C.R.M. Bangham, Population dynamics of immune responses to persistent viruses, Science 272 (1996) 74–79.
[23] M.A. Nowak, S. Bonhoeffer, Scientific correspondence, Science 375 (1995) 193.
[24] M.A. Nowak, R.M. May, Virus Dynamics: Mathematical Principles of Immunology and Virology, Oxford University Press, New York, 2000.
[25] M.A. Nowak, R.M. May, K. Sigmund, Immune-responses against multiple epitopes, Journal of Theoretical Biology 175 (1995) 325–353.
[26] D.A. Ouattara, Mathematical analysis of the HIV-1 infection: parameter estimation, therapies effectiveness and therapeutical failures, in: Proceedings of the 27th IEEE EMBS Annual International Conference, September 1–4, 2005, Shanghai, China.
[27] D.A. Ouattara, F. Bugnon, F. Raffi, C.H. Moog, Parameter identification of an HIV/AIDS model, in: Proceedings of the 13th International Symposium on HIV and Emerging Infectious Diseases, Toulon, France, 2004, September.
[28] A. S. Perelson, P. Essunger, M. Markowitz, D. D. Ho, How long should treatment be given if we had an antiretroviral regimen that completely blocked HIV replication?, in: Proceedings of the XIth International Conference on AIDS.
[29] A.S. Perelson, P. Essunger, et al., Decay characteristics of HIV-1 infected compartments during combination therapy, Nature 387 (1997) 188–191.
[30] A.S. Perelson, P.W. Nelson, Mathematical analysis of HIV-1 dynamics *in vivo*, SIAM Review 41 (1999) 3–44.
[31] A.S. Perelson, A.U. Neumann, M. Markowitz, J.M. Leonard, D.D. Ho, HIV-1 dynamics *in vivo*: virion clearance rate, infected cell life-span, and viral generation time, Science 271 (1996) 1582–1586.
[32] T.W. Schacker, J.P. Hughes, et al., Biological and virologic characteristics of primary HIV infection, Annals of Internal Medicine 128 (1998) 613–620.
[33] R. Schuurman, D. Descamps, et al., Multicenter comparison of three commercial methods for quantification of human immunodeficiency virus type 1 RNA in plasma, Journal of Clinical Microbiology 34 (1996) 3016–3022.
[34] W.Y. Tan, H. Wu, Stochastic modeling of the dynamics of $CD4^+$ T-cells by HIV and some Monte Carlo studies, Mathematical Biosciences 147 (1998) 173–205.
[35] USPHS, Guidelines for the use of antiretroviral agents in HIV-infected adults and adolescents. HIV/AIDS Treatment Information Service, 2003, http://www.aidsinfo.nih.gov.
[36] X. Wei, S.K. Ghosh, et al., Viral dynamics in HIV-1 infection, Nature 273 (1995) 112–117.
[37] H. Wu, W.Y. Tan, Deterministic and Stochastic Models of AIDS and HIV with Intervention, World Scientific, Publications, Singapore, 2005.
[38] X. Xia, Estimation of HIV/AIDS parameters, Automatica 39 (2003) 1983–1988.
[39] X. Xia, C.H. Moog, Identifiability of nonlinear systems with application to HIV/AIDS models, IEEE Transactions on Automatic Control 48 (2003) 330–336.